PROCEEDINGS OF SCIENCE

A new cross-check and review of aerosol attenuation measurements at the Pierre Auger Observatory

Violet M. Harvey[a,*] **for the Pierre Auger Collaboration**[b]

[a] *Department of Physics, The University of Adelaide, Adelaide, SA 5005, Australia*
[b] *Observatorio Pierre Auger, Av. San Martín Norte 304, 5613 Malargüe, Argentina*
Full author list: https://www.auger.org/archive/authors_icrc_2023.html

E-mail: spokespersons@auger.org

The distribution of aerosols in the atmosphere above cosmic ray fluorescence detectors must be well characterised in order to precisely recover extensive air shower properties such as the calorimetric energy, E, and depth of shower maximum, $X_{\rm max}$. The Pierre Auger Observatory uses two centrally located laser facilities to measure the vertical aerosol optical depth profile (VAOD) every hour. It is assumed that the night with the clearest atmosphere each year is effectively aerosol free and that it is an appropriate reference to set the absolute scale of VAOD throughout that year. We review the successes of this method and its associated sources of systematic uncertainty, then present a new cross-check of measured VAOD using air shower events observed in stereo mode. Special attention is paid to quantifying the uncertainties on this result. As the technique is only sensitive to VAOD bias at a fixed altitude, we combine it with a study of aerosol profiles independently measured using a less-sensitive Raman lidar system. This allows us to derive a complete model of the upper limit on the possible bias in the average measured VAOD, which we attribute primarily to an uncertainty on whether the annual reference nights are completely aerosol free. We formulate a correction for this bias and apply it retroactively to all VAOD measurements, then repeat the analysis of the complete air shower dataset and discuss the small but significant effect of this new correction on E and $X_{\rm max}$. This correction is now fully integrated into the Auger analysis chain.

38th International Cosmic Ray Conference (ICRC2023)
26 July – 3 August, 2023
Nagoya, Japan

*Speaker

PoS(ICRC2023)300

1. Introduction

The Pierre Auger Observatory [1] is located at approximately 1400 m above sea level (ASL) in the Mendoza province of Argentina. The surface detector array (SD) covers 3000 km^2 and is overlooked by the fluorescence detector (FD), composed of 27 fluorescence telescopes distributed across four sites. The observatory operates in a "hybrid" mode, where the SD can be used to improve the geometrical reconstruction of the FD observations. The atmosphere acts as a calorimeter for the FD, however the air fluorescence technique is very sensitive to the fraction of light scattered out of an air shower and attenuated along the path towards the detector. As such it is vital that the molecular (air pressure, temperature, and humidity) and aerosol properties are closely monitored. Near the centre of the surface array are two laser facilities, which each fire 200 vertical laser shots over the course of each hour. The track of laser light in the atmosphere is observed by the FD and this is used to derive the distribution of aerosols. We previously demonstrated the importance of measuring the vertical aerosol optical depth profile (VAOD or $\tau_{\mathrm{aer}}(h)$) on an hourly basis in [2]. The average degradation in air shower energy resolution without hourly aerosol measurements is a complex effect of a few per cent around 10^{18} eV but up to 20 % at the highest energies.

VAOD is measured with the data-normalised (DN) method [3], whereby the clearest night each year is assumed to have negligible aerosol content and is used as a reference to normalise all other laser observations from that year. This makes the analysis independent of the absolute calibration of the FD and laser, but sensitive to how well the calibration is tracked over a ±6 month period, as well as on how close the reference nights come to being truly aerosol free. Previously, the systematic uncertainty in the calibration tracking has been the dominant component and no uncertainty attributed to the reference night aerosol loading. The objective of this work was a data-driven cross-check of the DN aerosol results, culminating in an upper limit on the average bias in VAOD. This possible bias is ultimately attributed to reference night aerosols, and handled with a new VAOD correction and update to the systematic uncertainties.

2. The stereo energy balance technique

2.1 Definition and data selection

This technique was first described and used by Abbasi et al. [4] and further developed within the Pierre Auger Collaboration by Malacari [5]. It is based on air shower events observed simultaneously by at least two FD sites (so called "stereo" observations), and the expectation that along the segment of the shower track common to the views of both sites the reconstructed energy deposit should be consistent. The molecular component of the atmosphere is assumed to be well described by Rayleigh scattering theory, so the energy balance can be applied as a cross-check of the aerosol model and used to estimate the correction required if VAOD is systematically biased.

With reference to Fig. 1, let X_{A} and X_{B} be the start and end of the common segment of observed shower track, and D_k be the average distance to the common segment of track for the kth site. The reconstructed energy deposit along the common segment for each site is given by

$$\phi_k = \int_{X_{\mathrm{A}}}^{X_{\mathrm{B}}} \left(\frac{\mathrm{d}E}{\mathrm{d}X}\right)_k \mathrm{d}X \tag{1}$$

for $\frac{\mathrm{d}E}{\mathrm{d}X}$ the fitted Gaisser–Hillas shower profile. The energy balance is defined by the metric Ψ and abscissa ΔD,

$$\Psi = \frac{\phi_1 - \phi_2}{\frac{1}{2}(\phi_1 + \phi_2)} \qquad \Delta D = D_1 - D_2 \qquad (2)$$

which are the relative difference in reconstructed energy deposit along the common segment and the absolute difference in distances to the segment, respectively. The order of FD sites is kept the same when calculating these differences, to exploit the natural distribution of showers along the line of sight between any two sites. This ensures a distribution of ΔD including both positive and negative values and thus the longest possible lever arm for a linear fit. A negative slope in the relationship between Ψ and ΔD can be interpreted as an underestimation of the aerosol content of the atmosphere, because showers further away from one detector are inferred to have a lower energy than the same shower seen by a nearby detector. The uncertainty in the metric is obtained by propagating the uncertainties on ϕ_k which in turn arise from the Gaisser–Hillas function fit and the measurement uncertainty on each bin of the energy deposit profile. For our analysis we selected hybrid events with long tracks, X_{max} in the field of view, and good quality Gaisser–Hillas fits, observed between 2004 and 2018. According to the atmospheric monitoring instruments [2] the events were unaffected by clouds. For a shower observed at more than two sites, all unique pairs were formed as independent data points. 673 stereo pairs were formed by the events surviving cuts.

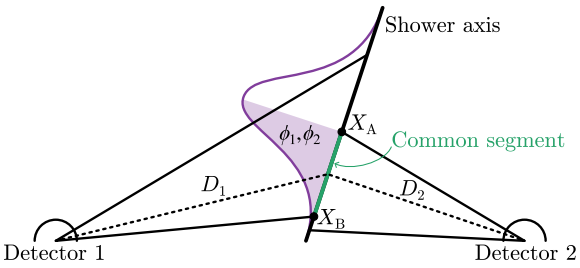

Figure 1: Variables relevant to the stereo energy balance. Solid lines emanating from each detector indicate the field of view.

2.2 Search for the mean bias in VAOD

The stereo energy balance was produced in two steps. First, the data were split into subsets by FD site combination and linear fits performed to the distribution of Ψ versus ΔD for each subset. This revealed that the subsets had comparable slopes but unique non-zero y-intercepts, henceforth "Ψ offsets". These offsets are caused by systematic differences in the calibration of each FD site, which influence the count of photons at each detector in a fractional sense *independent* of distance to the shower, and thereby have no effect on the slope. These variations in calibration between FD sites are small and within the expected systematic uncertainties. However, they induce a broadening in Ψ in the combined dataset and if unaddressed would reduce the precision of the fitted slope. As such, the second step of the procedure was to subtract the Ψ offset of each subset from the points in that subset, before a linear fit was performed to the combined set. The linear fits to each subset after Ψ offset subtraction are shown in Fig. 2a, while the fit for the complete dataset is shown in Fig. 2b. Empirically, it was determined that the metric uncertainties had to be increased by a factor of two to bring the χ^2 of the linear fit down to match the number of degrees of freedom. This was expected as there are some sources of random atmospheric uncertainty – for instance, the horizontal uniformity of aerosols across the array – that are not present in the analysis at the level of the Gaisser–Hillas fit. The energy balance of the combined set exhibited a slope of $(-0.22 \pm 0.04)\,\%\,\mathrm{km}^{-1}$, indicating aerosol underestimation equivalent to showers at a typical distance of 20 km to 25 km from the FD having energy deposits underestimated by up to 5 %.

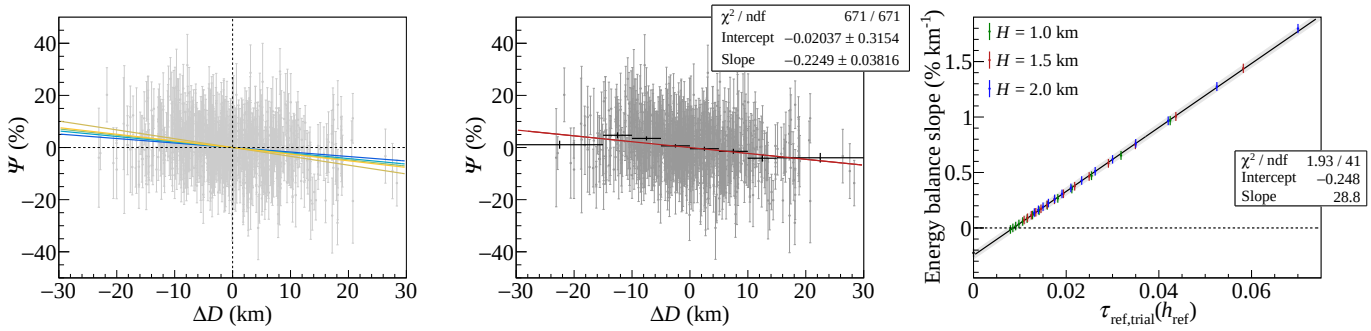

(a) Stereo energy balance for each subset after Ψ offset subtraction.

(b) Stereo energy balance for the combined set.

(c) Stereo energy balance slope as a function of trial reference night VAOD.

Figure 2: Key results from the stereo energy balance analysis. In panel (a), fits are shown for five of the six FD site combinations with the sixth combination excluded as it has only three data points. In panel (b), the profile bins are for visualisation only. Error bars on the profile bins show the standard error of the mean. In panel (c), the grey shaded region indicates the uncertainty band on the fit from moving all points ±1 σ and repeating the fit. See text for further interpretation of the plots.

We sought to determine the amount by which the VAOD would have to be underestimated on average to produce the observed effect, which will be referred to simply as reference night aerosols. The true VAOD for any hour is equivalent to the sum of the observed VAOD for that hour and the VAOD that was present on the reference night: $\tau_{\text{true}}(h) = \tau_{\text{DN}}(h) + \tau_{\text{ref}}(h)$. Assuming that the reference night aerosol distribution could be described by a two-parameter exponential model,

$$\tau_{\text{ref}}(h) = \frac{H_{\text{aer}}}{L_{\text{aer}}}\left(1 - \mathrm{e}^{-\frac{h}{H_{\text{aer}}}}\right), \tag{3}$$

we sought the scale height, H_{aer}, and attenuation length at ground, L_{aer}, of the average reference night. This was achieved by modifying the VAOD for each stereo shower by adding a trial $\tau_{\text{ref}}(h)$, and seeking the parameters H_{aer} and L_{aer} required to make the slope of the stereo energy balance in the repeated reconstruction consistent with zero. A range of values for H_{aer} and L_{aer} were considered to produce an ensemble of 43 trial reference night aerosol distributions, $\tau_{\text{ref,trial}}(h)$. Fig. 2c plots energy balance slope against the trial reference night VAOD at the reference height, h_{ref}, of 4.5 km ASL. The change in energy balance slope was found to be independent of the H_{aer} chosen for the trial reference night VAOD. A linear fit was performed to the full ensemble of points. Propagation of the energy balance fit uncertainties to the linear fit was performed by coherently shifting all points in the ensemble ±1 σ and repeating the linear fit again at each position. From the intercept of the fit with zero, a value of $\tau_{\text{ref}}(h_{\text{ref}}) = 0.009 \pm 0.001$ was concluded to represent the collective underestimation of the VAOD. The uncertainty presented here is predominantly due to the measurement uncertainty in Ψ, which in turn arises from statistical uncertainties in the event reconstruction. The uncertainty should be interpreted as the standard error of the mean reference night VAOD, rather than producing any insight into the variation of the reference night VAOD over time.

2.3 Quantification of systematic uncertainties

Tests were performed to estimate the effect of four sources of systematic uncertainty in the stereo energy balance technique, the methodology and results of which are summarised here.

Intrinsic biases of the stereo energy balance technique were assessed using air shower simulations, where the true value of $\tau_{\text{ref}}(h_{\text{ref}})$ could be controlled. The 631 air showers that form the 673 stereo pairs were simulated with CONEX, configured to match their observed energy and geometry. The Auger FD simulation was configured to match the real conditions at the time of each shower observation as closely as possible. X_{max} could not be controlled in CONEX, so multiple realisations of the 631-event dataset were prepared to ensure that the same source event was simulated with a variety of X_{max} following a distribution comparable with real data. Air showers were simulated in the "true" atmosphere of $\tau_{\text{true}}(h) = \tau_{\text{DN}}(h) + \tau_{\text{ref}}(h)$ for a variety of $\tau_{\text{ref}}(h)$ and reconstructed in the "measured" atmosphere of $\tau_{\text{meas}}(h) = \tau_{\text{DN}}(h)$. After analysing these events with the stereo energy balance, a bias in the recovered $\tau_{\text{ref}}(h_{\text{ref}})$ of 0.003 ± 0.001 was found. The bias has an uncertainty due to the variation in X_{max} of the same event across different realisations.

The curved FD mirrors slowly accumulate dust primarily at the bottom of each mirror, and are irregularly cleaned to remove it. The design of the telescopes means light arriving from different viewing elevations encounters different amounts of dust, and stereo air showers that are closer to one FD site than another appear higher in elevation at the telescope they are closest to, hence suffering additional unaccounted-for light losses. We developed a first-order correction for the attenuating effect of dust on stereo air showers, which had the effect of increasing the inferred energy deposit of showers that landed closer to a telescope. This caused a decrease in energy balance slope and $\tau_{\text{ref}}(h_{\text{ref}})$ was found to increase by 0.002. To account for the *ad hoc* nature of this correction we chose to treat the result as a bias correction of $+0.001 \pm 0.001$.

For distant air showers, some light will arrive at the FD later than other light that was emitted from the same point on the shower axis because of multiple scattering [6]. This is typically corrected for by scaling down the intensity of energy deposit bins to eliminate additional photons and focus exclusively on singly scattered light. Any bias in the calculation of the correction may translate to a bias in the energy balance slope because more distant showers are more affected. The Auger Collaboration does not quote a systematic uncertainty on the multiple scattering correction, so for a conservative assessment an uncertainty of $\pm 50\,\%$ was assumed. After repeating the reconstruction of the relevant stereo events with the multiple-scattering fraction increased or decreased accordingly, the measured $\tau_{\text{ref}}(h_{\text{ref}})$ was found to change by ± 0.002.

The lateral width correction accounts for light arriving at the FD camera outside of the integration region, caused by the intrinsic air shower width and optical point spread function of the telescope [7]. This effect is most significant for nearby showers, and in the standard analysis is corrected for by scaling up the energy deposit profile based on a simulation-driven model. In the same fashion as for the multiple scattering correction, the impact of a systematic in the lateral width correction was assessed by applying the correction at $\pm 50\,\%$ of its typical magnitude. The measured $\tau_{\text{ref}}(h_{\text{ref}})$ was observed to differ by only ± 0.0003. This result being so small is attributed to the stereo events being at sufficient distances that the correction changes little.

The influences of each of these systematic effects on $\tau_{\text{ref}}(h_{\text{ref}})$ are collated in Tab. 1. Combining components in quadrature, the final measurement of the mean bias in VAOD comes to $0.007 \pm$

	$\tau_{\mathrm{ref}}(h_{\mathrm{ref}})$
Initial result	0.009 ± 0.001
Correction of intrinsic bias	−0.003 ± 0.001
Correction of FD mirror dust	+0.001 ± 0.001
Multiple scattering correction ±50 %	± 0.002
Lateral width correction ±50 %	± 0.0003

Table 1: Summary of all systematic influences on the stereo energy balance result.

0.001 (stat.) ± 0.002 (sys.). Acknowledging that other, unassessed, systematic effects may influence the stereo energy balance technique, we chose to use this measurement as the basis of a conservative upper limit on the possible systematic bias in VAOD, and presume reference night aerosols to be the primary contribution to this bias. The 1 σ upper limit of the measurement, $\tau^{\mathrm{up}}_{\mathrm{ref}}(h_{\mathrm{ref}}) = 0.01$, was used for this systematic uncertainty component. For comparison, the mean VAOD at h_{ref}, prior to the correction from this work, is 0.04. This upper limit on the bias is therefore relatively small and demonstrates the accuracy of the DN method.

3. Reference night aerosol scale height

As previously noted, the stereo energy balance could not probe the distribution of aerosols due to restrictions of the event geometry. As such, an alternate method was required to interrogate H_{aer}, and for this the Raman lidar was chosen. The Auger Raman lidar [8] measures the N_2 Raman backscatter signal, among other properties, three times each night, from which the VAOD can be evaluated. Reference nights push the limit of observational ability for Raman lidar, which rule out direct measurement of reference night VAOD. However, these systematics do not so much affect the "shape" of the profiles, making them still a fine choice for studying the distribution of aerosols at low altitudes.

Eight years of Raman lidar data were analysed, with Eq. 3 fitted to the VAOD profiles in the range from 0.7 km to 6 km AGL. This avoided an instrumental bias region at low altitude and possible clouds at high altitude, while still covering the region in which the majority of aerosols can be expected to be encountered. Quality cuts based on the goodness of fit excluded any profiles that were likely to have been affected by cloud, after which remained 1072 fits for further study. Two subsets of the data were selected: a "summer" subset comprising ~250 events from December–February, and a "winter" subset of the same size for June–August. Almost every reference night used by the DN method falls within the austral winter. Fig. 3a shows the fitted H_{aer} plotted against the fitted $\tau_{\mathrm{aer}}(h_{\mathrm{ref}})$. H_{aer} is seen to exhibit a seasonal dependence, reaching lower values in winter and higher values in summer. No particular dependence on VAOD is observed, as the relationship of H_{aer} with $\tau_{\mathrm{aer}}(h_{\mathrm{ref}})$ is quite flat. This indicates that the scale height on reference nights – which are among the nights with the lowest aerosol loading – does not behave in any way differently to the scale height on nights with much higher aerosol loading. From this it was inferred that reference nights could be treated the same as all other nights when it came to estimating the average scale height. Fig. 3b shows the distributions of fitted H_{aer} for the summer and winter subsets, from which the mean winter scale height, and hence reference night scale height, is seen to be $H_{\mathrm{aer}} = 1.5$ km.

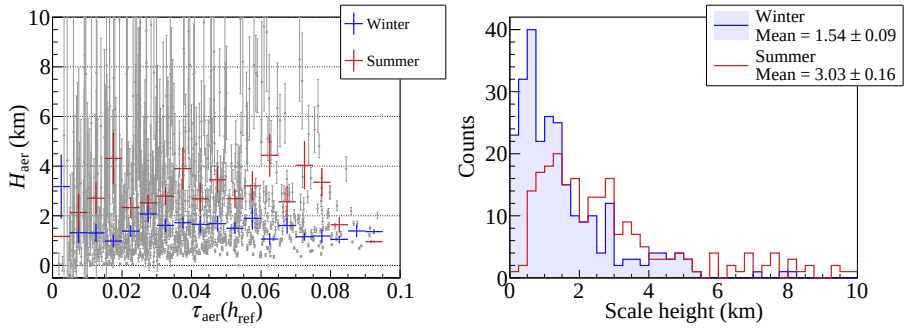

(a) Fitted H_{aer} vs. fitted $\tau_{aer}(h_{ref})$. **(b)** Fitted H_{aer} for each season.

Figure 3: Fit parameters of good-quality Raman lidar aerosol profiles. In panel (a), grey points show fit results from all seasons, while coloured profile bins show only the seasonal subsets. Error bars on the profile bins show the standard error of the mean.

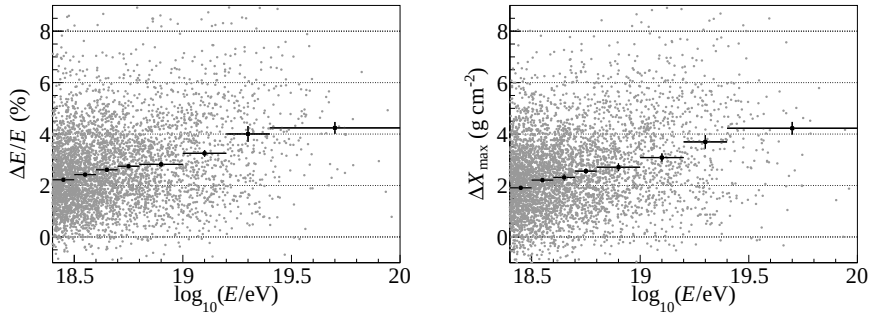

Figure 4: Changes in air shower energy (left) and X_{max} (right) after application of the reference night aerosol correction. Error bars show the standard error of the mean.

4. The reference night aerosol correction

The result of the stereo energy balance cross-check was an upper limit of 0.01 on the potential systematic bias in VAOD at h_{ref}. We created a new VAOD uncertainty component to account for this systematic by applying a VAOD correction of $\tau_{aer}(h_{ref}) = 0.005 \pm 0.005$ with scale height $H_{aer} = 1.5$ km. This increases all VAOD measurements while also setting the systematic uncertainty on VAOD to at least ±0.005 at h_{ref}. The new VAOD systematic uncertainty is larger than 0.005 due to the consideration of the FD and laser calibration systematics, but overall still smaller than its historical value. We applied the correction and renewal of systematic uncertainties to the complete database of VAOD measurements at Auger. Changes to E and X_{max} with the new VAOD database are small but significant. Fig. 4 shows the changes in air shower energy and depth of shower maximum. Energy increases by 2 % to 4 % on average across the range from 3×10^{18} eV to 10^{20} eV, while X_{max} increases by 2 g cm^{-2} to 4 g cm^{-2}. Fig. 5 shows the new systematic uncertainties in these parameters due to aerosols. The new systematic uncertainty on energy is 2 % to 4 %, which is smaller than the previous 3 % to 6 % [7]. This decrease can be attributed to an improved understanding of the magnitude of relevant uncertainty sources. The previous systematic uncertainty on X_{max} due to aerosols was a few per cent, and the new systematic uncertainty is comparable to this.

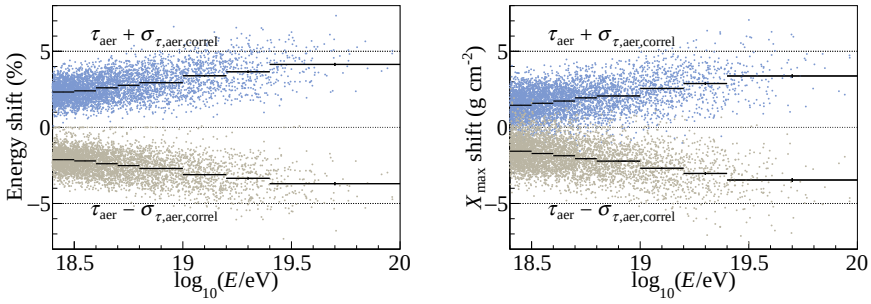

Figure 5: New systematic uncertainties in air shower energy (left) and X_{max} (right) after renewal of the VAOD correlated (systematic) uncertainty to include reference night aerosols. Error bars show the standard error of the mean.

5. Conclusion

The stereo energy balance technique was used to place an upper limit of 0.01 on the mean bias in VAOD at 4.5 km ASL, which is due to an uncertainty on whether the reference nights used by the data-normalised method are aerosol free. A separate study of aerosol profiles from the independent Raman lidar system inferred the mean scale height of aerosols on reference nights. These were combined to create a reference night aerosol correction. The VAOD can be said to be within 0.005 of the true value on average, the mean VAOD (after correction) being 0.045. The reference night aerosol correction is now integrated into the standard analysis and will be present in all Auger results going forward, including those in these proceedings. Further studies are pending to cross-check this analysis which may be able to further refine the applied correction. An upcoming publication will provide more detail on the reviewed systematic uncertainties and the manner in which the influence of reference night aerosols was taken into account on statistical uncertainties as well.

Acknowledgments

This work was supported with supercomputing resources provided by the Phoenix HPC service at the University of Adelaide. The author thanks the Australian Institute of Physics Student Travel Award and the Astronomical Society of Australia Student Travel Assistance Scheme for their support.

References

[1] A. Aab et al. (Pierre Auger Collaboration), Nucl. Instrum. Methods Phys. Res., Sect. A **798**, 172 (2015).

[2] V. M. Harvey (for the Pierre Auger Collaboration), PoS **ICRC2019**, 283 (2019).

[3] P. Abreu et al. (Pierre Auger Collaboration), J. Instrum. **8**, P04009 (2013).

[4] R. U. Abbasi et al. (High Resolution Fly's Eye Collaboration), Astropart. Phys. **25**, 93 (2006).

[5] M. Malacari, PhD thesis (The University of Adelaide, 2016), HDL: 2440/103620.

[6] J. Abraham et al. (Pierre Auger Collaboration), Astropart. Phys. **33**, 108 (2010), arXiv:1002.0366 [astro-ph.IM].

[7] V. Verzi (for the Pierre Auger Collaboration), Proc. Int. Cosm. Ray Conf. (2013), arXiv:1307.5059 [astro-ph.HE].

[8] V. Rizi et al. (for the Pierre Auger Collaboration), EPJ Web Conf. **197**, 02003 (2019).

The Pierre Auger Collaboration

A. Abdul Halim[13], P. Abreu[72], M. Aglietta[54,52], I. Allekotte[1], K. Almeida Cheminant[70], A. Almela[7,12], R. Aloisio[45,46], J. Alvarez-Muñiz[79], J. Ammerman Yebra[79], G.A. Anastasi[54,52], L. Anchordoqui[86], B. Andrada[7], S. Andringa[72], C. Aramo[50], P.R. Araújo Ferreira[42], E. Arnone[63,52], J. C. Arteaga Velázquez[67], H. Asorey[7], P. Assis[72], G. Avila[11], E. Avocone[57,46], A.M. Badescu[75], A. Bakalova[32], A. Balaceanu[73], F. Barbato[45,46], A. Bartz Mocellin[85], J.A. Bellido[13,69], C. Berat[36], M.E. Bertaina[63,52], G. Bhatta[70], M. Bianciotto[63,52], P.L. Biermann[h], V. Binet[5], K. Bismark[39,7], T. Bister[80,81], J. Biteau[37], J. Blazek[32], C. Bleve[36], J. Blümer[41], M. Boháčová[32], D. Boncioli[57,46], C. Bonifazi[8,26], L. Bonneau Arbeletche[21], N. Borodai[70], J. Brack[j], P.G. Brichetto Orchera[7], F.L. Briechle[42], A. Bueno[78], S. Buitink[15], M. Buscemi[47,61], M. Büsken[39,7], A. Bwembya[80,81], K.S. Caballero-Mora[66], S. Cabana-Freire[79], L. Caccianiga[59,49], I. Caracas[38], R. Caruso[58,47], A. Castellina[54,52], F. Catalani[18], G. Cataldi[48], L. Cazon[79], M. Cerda[10], A. Cermenati[45,46], J.A. Chinellato[21], J. Chudoba[32], L. Chytka[33], R.W. Clay[13], A.C. Cobos Cerutti[6], R. Colalillo[60,50], A. Coleman[90], M.R. Coluccia[48], R. Conceição[72], A. Condorelli[37], G. Consolati[49,55], M. Conte[56,48], F. Convenga[41], D. Correia dos Santos[28], P.J. Costa[72], C.E. Covault[84], M. Cristinziani[44], C.S. Cruz Sanchez[3], S. Dasso[4,2], K. Daumiller[41], B.R. Dawson[13], R.M. de Almeida[28], J. de Jesús[7,41], S.J. de Jong[80,81], J.R.T. de Mello Neto[26,27], I. De Mitri[45,46], J. de Oliveira[17], D. de Oliveira Franco[21], F. de Palma[56,48], V. de Souza[19], E. De Vito[56,48], A. Del Popolo[58,47], O. Deligny[34], N. Denner[32], L. Deval[41,7], A. di Matteo[52], M. Dobre[73], C. Dobrigkeit[21], J.C. D'Olivo[68], L.M. Domingues Mendes[72], J.C. dos Anjos, R.C. dos Anjos[25], J. Ebr[32], F. Ellwanger[41], M. Emam[80,81], R. Engel[39,41], I. Epicoco[56,48], M. Erdmann[42], A. Etchegoyen[7,12], C. Evoli[45,46], H. Falcke[80,82,81], J. Farmer[89], G. Farrar[88], A.C. Fauth[21], N. Fazzini[e], F. Feldbusch[40], F. Fenu[41,d], A. Fernandes[72], B. Fick[87], J.M. Figueira[7], A. Filipčič[77,76], T. Fitoussi[41], B. Flaggs[90], T. Fodran[80], T. Fujii[89,f], A. Fuster[7,12], C. Galea[80], C. Galelli[59,49], B. García[6], C. Gaudu[38], H. Gemmeke[40], F. Gesualdi[7,41], A. Gherghel-Lascu[73], P.L. Ghia[34], U. Giaccari[48], M. Giammarchi[49], J. Glombitza[42,g], F. Gobbi[10], F. Gollan[7], G. Golup[1], M. Gómez Berisso[1], P.F. Gómez Vitale[11], J.P. Gongora[11], J.M. González[1], N. González[7], I. Goos[1], D. Góra[70], A. Gorgi[54,52], M. Gottowik[79], T.D. Grubb[13], F. Guarino[60,50], G.P. Guedes[22], E. Guido[44], S. Hahn[39], P. Hamal[32], M.R. Hampel[7], P. Hansen[3], D. Harari[1], V.M. Harvey[13], A. Haungs[41], T. Hebbeker[42], C. Hojvat[e], J.R. Hörandel[80,81], P. Horvath[33], M. Hrabovský[33], T. Huege[41,15], A. Insolia[58,47], P.G. Isar[74], P. Janecek[32], J.A. Johnsen[85], J. Jurysek[32], A. Kääpä[38], K.H. Kampert[38], B. Keilhauer[41], A. Khakurdikar[80], V.V. Kizakke Covilakam[7,41], H.O. Klages[41], M. Kleifges[40], F. Knapp[39], N. Kunka[40], B.L. Lago[16], N. Langner[42], M.A. Leigui de Oliveira[24], Y Lema-Capeans[79], V. Lenok[39], A. Letessier-Selvon[35], I. Lhenry-Yvon[34], D. Lo Presti[58,47], L. Lopes[72], L. Lu[91], Q. Luce[39], J.P. Lundquist[76], A. Machado Payeras[21], M. Majercakova[32], D. Mandat[32], B.C. Manning[13], P. Mantsch[e], S. Marafico[34], F.M. Mariani[59,49], A.G. Mariazzi[3], I.C. Mariş[14], G. Marsella[61,47], D. Martello[56,48], S. Martinelli[41,7], O. Martínez Bravo[64], M.A. Martins[79], M. Mastrodicasa[57,46], H.J. Mathes[41], J. Matthews[a], G. Matthiae[62,51], E. Mayotte[85,38], S. Mayotte[85], P.O. Mazur[e], G. Medina-Tanco[68], J. Meinert[38], D. Melo[7], A. Menshikov[40], C. Merx[41], S. Michal[33], M.I. Micheletti[5], L. Miramonti[59,49], S. Mollerach[1], F. Montanet[36], L. Morejon[38], C. Morello[54,52], A.L. Müller[32], K. Mulrey[80,81], R. Mussa[52], M. Muzio[88], W.M. Namasaka[38], S. Negi[32], L. Nellen[68], K. Nguyen[87], G. Nicora[9], M. Niculescu-Oglinzanu[73], M. Niechciol[44], D. Nitz[87], D. Nosek[31], V. Novotny[31], L. Nožka[33], A Nucita[56,48], L.A. Núñez[30], C. Oliveira[19], M. Palatka[32], J. Pallotta[9], S. Panja[32], G. Parente[79], T. Paulsen[38], J. Pawlowsky[38], M. Pech[32], J. Pękala[70], R. Pelayo[65], L.A.S. Pereira[23], E.E. Pereira Martins[39,7], J. Perez Armand[20], C. Pérez Bertolli[7,41], L. Perrone[56,48], S. Petrera[45,46], C. Petrucci[57,46], T. Pierog[41], M. Pimenta[72], M. Platino[7], B. Pont[80], M. Pothast[81,80], M. Pourmohammad Shahvar[61,47], P. Privitera[89], M. Prouza[32], A. Puyleart[87], S. Querchfeld[38], J. Rautenberg[38], D. Ravignani[7], M. Reininghaus[39], J. Ridky[32], F. Riehn[79], M. Risse[44], V. Rizi[57,46], W. Rodrigues de Carvalho[80], E. Rodriguez[7,41], J. Rodriguez Rojo[11], M.J. Roncoroni[7], S. Rossoni[43], M. Roth[41], E. Roulet[1], A.C. Rovero[4], P. Ruehl[44], A. Saftoiu[73], M. Saharan[80], F. Salamida[57,46], H. Salazar[64], G. Salina[51], J.D. Sanabria Gomez[30], F. Sánchez[7], E.M. Santos[20], E. Santos[32],

F. Sarazin[85], R. Sarmento[72], R. Sato[11], P. Savina[91], C.M. Schäfer[41], V. Scherini[56,48], H. Schieler[41], M. Schimassek[34], M. Schimp[38], F. Schlüter[41], D. Schmidt[39], O. Scholten[15,i], H. Schoorlemmer[80,81], P. Schovánek[32], F.G. Schröder[90,41], J. Schulte[42], T. Schulz[41], S.J. Sciutto[3], M. Scornavacche[7,41], A. Segreto[53,47], S. Sehgal[38], S.U. Shivashankara[76], G. Sigl[43], G. Silli[7], O. Sima[73,b], F. Simon[40], R. Smau[73], R. Šmída[89], P. Sommers[k], J.F. Soriano[86], R. Squartini[10], M. Stadelmaier[32], D. Stanca[73], S. Stanič[76], J. Stasielak[70], P. Stassi[36], S. Strähnz[39], M. Straub[42], M. Suárez-Durán[14], T. Suomijärvi[37], A.D. Supanitsky[7], Z. Svozilikova[32], Z. Szadkowski[71], A. Tapia[29], C. Taricco[63,52], C. Timmermans[81,80], O. Tkachenko[41], P. Tobiska[32], C.J. Todero Peixoto[18], B. Tomé[72], Z. Torrès[36], A. Travaini[10], P. Travnicek[32], C. Trimarelli[57,46], M. Tueros[3], M. Unger[41], L. Vaclavek[33], M. Vacula[33], J.F. Valdés Galicia[68], L. Valore[60,50], E. Varela[64], A. Vásquez-Ramírez[30], D. Veberič[41], C. Ventura[27], I.D. Vergara Quispe[3], V. Verzi[51], J. Vicha[32], J. Vink[83], J. Vlastimil[32], S. Vorobiov[76], C. Watanabe[26], A.A. Watson[c], A. Weindl[41], L. Wiencke[85], H. Wilczyński[70], D. Wittkowski[38], B. Wundheiler[7], B. Yue[38], A. Yushkov[32], O. Zapparrata[14], E. Zas[79], D. Zavrtanik[76,77], M. Zavrtanik[77,76]

———— • ————

[1] Centro Atómico Bariloche and Instituto Balseiro (CNEA-UNCuyo-CONICET), San Carlos de Bariloche, Argentina
[2] Departamento de Física and Departamento de Ciencias de la Atmósfera y los Océanos, FCEyN, Universidad de Buenos Aires and CONICET, Buenos Aires, Argentina
[3] IFLP, Universidad Nacional de La Plata and CONICET, La Plata, Argentina
[4] Instituto de Astronomía y Física del Espacio (IAFE, CONICET-UBA), Buenos Aires, Argentina
[5] Instituto de Física de Rosario (IFIR) – CONICET/U.N.R. and Facultad de Ciencias Bioquímicas y Farmacéuticas U.N.R., Rosario, Argentina
[6] Instituto de Tecnologías en Detección y Astropartículas (CNEA, CONICET, UNSAM), and Universidad Tecnológica Nacional – Facultad Regional Mendoza (CONICET/CNEA), Mendoza, Argentina
[7] Instituto de Tecnologías en Detección y Astropartículas (CNEA, CONICET, UNSAM), Buenos Aires, Argentina
[8] International Center of Advanced Studies and Instituto de Ciencias Físicas, ECyT-UNSAM and CONICET, Campus Miguelete – San Martín, Buenos Aires, Argentina
[9] Laboratorio Atmósfera – Departamento de Investigaciones en Láseres y sus Aplicaciones – UNIDEF (CITEDEF-CONICET), Argentina
[10] Observatorio Pierre Auger, Malargüe, Argentina
[11] Observatorio Pierre Auger and Comisión Nacional de Energía Atómica, Malargüe, Argentina
[12] Universidad Tecnológica Nacional – Facultad Regional Buenos Aires, Buenos Aires, Argentina
[13] University of Adelaide, Adelaide, S.A., Australia
[14] Université Libre de Bruxelles (ULB), Brussels, Belgium
[15] Vrije Universiteit Brussels, Brussels, Belgium
[16] Centro Federal de Educação Tecnológica Celso Suckow da Fonseca, Petropolis, Brazil
[17] Instituto Federal de Educação, Ciência e Tecnologia do Rio de Janeiro (IFRJ), Brazil
[18] Universidade de São Paulo, Escola de Engenharia de Lorena, Lorena, SP, Brazil
[19] Universidade de São Paulo, Instituto de Física de São Carlos, São Carlos, SP, Brazil
[20] Universidade de São Paulo, Instituto de Física, São Paulo, SP, Brazil
[21] Universidade Estadual de Campinas, IFGW, Campinas, SP, Brazil
[22] Universidade Estadual de Feira de Santana, Feira de Santana, Brazil
[23] Universidade Federal de Campina Grande, Centro de Ciencias e Tecnologia, Campina Grande, Brazil
[24] Universidade Federal do ABC, Santo André, SP, Brazil
[25] Universidade Federal do Paraná, Setor Palotina, Palotina, Brazil
[26] Universidade Federal do Rio de Janeiro, Instituto de Física, Rio de Janeiro, RJ, Brazil
[27] Universidade Federal do Rio de Janeiro (UFRJ), Observatório do Valongo, Rio de Janeiro, RJ, Brazil
[28] Universidade Federal Fluminense, EEIMVR, Volta Redonda, RJ, Brazil
[29] Universidad de Medellín, Medellín, Colombia
[30] Universidad Industrial de Santander, Bucaramanga, Colombia

[31] Charles University, Faculty of Mathematics and Physics, Institute of Particle and Nuclear Physics, Prague, Czech Republic
[32] Institute of Physics of the Czech Academy of Sciences, Prague, Czech Republic
[33] Palacky University, Olomouc, Czech Republic
[34] CNRS/IN2P3, IJCLab, Université Paris-Saclay, Orsay, France
[35] Laboratoire de Physique Nucléaire et de Hautes Energies (LPNHE), Sorbonne Université, Université de Paris, CNRS-IN2P3, Paris, France
[36] Univ. Grenoble Alpes, CNRS, Grenoble Institute of Engineering Univ. Grenoble Alpes, LPSC-IN2P3, 38000 Grenoble, France
[37] Université Paris-Saclay, CNRS/IN2P3, IJCLab, Orsay, France
[38] Bergische Universität Wuppertal, Department of Physics, Wuppertal, Germany
[39] Karlsruhe Institute of Technology (KIT), Institute for Experimental Particle Physics, Karlsruhe, Germany
[40] Karlsruhe Institute of Technology (KIT), Institut für Prozessdatenverarbeitung und Elektronik, Karlsruhe, Germany
[41] Karlsruhe Institute of Technology (KIT), Institute for Astroparticle Physics, Karlsruhe, Germany
[42] RWTH Aachen University, III. Physikalisches Institut A, Aachen, Germany
[43] Universität Hamburg, II. Institut für Theoretische Physik, Hamburg, Germany
[44] Universität Siegen, Department Physik – Experimentelle Teilchenphysik, Siegen, Germany
[45] Gran Sasso Science Institute, L'Aquila, Italy
[46] INFN Laboratori Nazionali del Gran Sasso, Assergi (L'Aquila), Italy
[47] INFN, Sezione di Catania, Catania, Italy
[48] INFN, Sezione di Lecce, Lecce, Italy
[49] INFN, Sezione di Milano, Milano, Italy
[50] INFN, Sezione di Napoli, Napoli, Italy
[51] INFN, Sezione di Roma "Tor Vergata", Roma, Italy
[52] INFN, Sezione di Torino, Torino, Italy
[53] Istituto di Astrofisica Spaziale e Fisica Cosmica di Palermo (INAF), Palermo, Italy
[54] Osservatorio Astrofisico di Torino (INAF), Torino, Italy
[55] Politecnico di Milano, Dipartimento di Scienze e Tecnologie Aerospaziali , Milano, Italy
[56] Università del Salento, Dipartimento di Matematica e Fisica "E. De Giorgi", Lecce, Italy
[57] Università dell'Aquila, Dipartimento di Scienze Fisiche e Chimiche, L'Aquila, Italy
[58] Università di Catania, Dipartimento di Fisica e Astronomia "Ettore Majorana", Catania, Italy
[59] Università di Milano, Dipartimento di Fisica, Milano, Italy
[60] Università di Napoli "Federico II", Dipartimento di Fisica "Ettore Pancini", Napoli, Italy
[61] Università di Palermo, Dipartimento di Fisica e Chimica "E. Segrè", Palermo, Italy
[62] Università di Roma "Tor Vergata", Dipartimento di Fisica, Roma, Italy
[63] Università Torino, Dipartimento di Fisica, Torino, Italy
[64] Benemérita Universidad Autónoma de Puebla, Puebla, México
[65] Unidad Profesional Interdisciplinaria en Ingeniería y Tecnologías Avanzadas del Instituto Politécnico Nacional (UPIITA-IPN), México, D.F., México
[66] Universidad Autónoma de Chiapas, Tuxtla Gutiérrez, Chiapas, México
[67] Universidad Michoacana de San Nicolás de Hidalgo, Morelia, Michoacán, México
[68] Universidad Nacional Autónoma de México, México, D.F., México
[69] Universidad Nacional de San Agustin de Arequipa, Facultad de Ciencias Naturales y Formales, Arequipa, Peru
[70] Institute of Nuclear Physics PAN, Krakow, Poland
[71] University of Łódź, Faculty of High-Energy Astrophysics,Łódź, Poland
[72] Laboratório de Instrumentação e Física Experimental de Partículas – LIP and Instituto Superior Técnico – IST, Universidade de Lisboa – UL, Lisboa, Portugal
[73] "Horia Hulubei" National Institute for Physics and Nuclear Engineering, Bucharest-Magurele, Romania
[74] Institute of Space Science, Bucharest-Magurele, Romania
[75] University Politehnica of Bucharest, Bucharest, Romania
[76] Center for Astrophysics and Cosmology (CAC), University of Nova Gorica, Nova Gorica, Slovenia
[77] Experimental Particle Physics Department, J. Stefan Institute, Ljubljana, Slovenia

PoS(ICRC2023)300

[78] Universidad de Granada and C.A.F.P.E., Granada, Spain
[79] Instituto Galego de Física de Altas Enerxías (IGFAE), Universidade de Santiago de Compostela, Santiago de Compostela, Spain
[80] IMAPP, Radboud University Nijmegen, Nijmegen, The Netherlands
[81] Nationaal Instituut voor Kernfysica en Hoge Energie Fysica (NIKHEF), Science Park, Amsterdam, The Netherlands
[82] Stichting Astronomisch Onderzoek in Nederland (ASTRON), Dwingeloo, The Netherlands
[83] Universiteit van Amsterdam, Faculty of Science, Amsterdam, The Netherlands
[84] Case Western Reserve University, Cleveland, OH, USA
[85] Colorado School of Mines, Golden, CO, USA
[86] Department of Physics and Astronomy, Lehman College, City University of New York, Bronx, NY, USA
[87] Michigan Technological University, Houghton, MI, USA
[88] New York University, New York, NY, USA
[89] University of Chicago, Enrico Fermi Institute, Chicago, IL, USA
[90] University of Delaware, Department of Physics and Astronomy, Bartol Research Institute, Newark, DE, USA
[91] University of Wisconsin-Madison, Department of Physics and WIPAC, Madison, WI, USA

—

[a] Louisiana State University, Baton Rouge, LA, USA
[b] also at University of Bucharest, Physics Department, Bucharest, Romania
[c] School of Physics and Astronomy, University of Leeds, Leeds, United Kingdom
[d] now at Agenzia Spaziale Italiana (ASI). Via del Politecnico 00133, Roma, Italy
[e] Fermi National Accelerator Laboratory, Fermilab, Batavia, IL, USA
[f] now at Graduate School of Science, Osaka Metropolitan University, Osaka, Japan
[g] now at ECAP, Erlangen, Germany
[h] Max-Planck-Institut für Radioastronomie, Bonn, Germany
[i] also at Kapteyn Institute, University of Groningen, Groningen, The Netherlands
[j] Colorado State University, Fort Collins, CO, USA
[k] Pennsylvania State University, University Park, PA, USA

Acknowledgments

The successful installation, commissioning, and operation of the Pierre Auger Observatory would not have been possible without the strong commitment and effort from the technical and administrative staff in Malargüe. We are very grateful to the following agencies and organizations for financial support:

Argentina – Comisión Nacional de Energía Atómica; Agencia Nacional de Promoción Científica y Tecnológica (ANPCyT); Consejo Nacional de Investigaciones Científicas y Técnicas (CONICET); Gobierno de la Provincia de Mendoza; Municipalidad de Malargüe; NDM Holdings and Valle Las Leñas; in gratitude for their continuing cooperation over land access; Australia – the Australian Research Council; Belgium – Fonds de la Recherche Scientifique (FNRS); Research Foundation Flanders (FWO); Brazil – Conselho Nacional de Desenvolvimento Científico e Tecnológico (CNPq); Financiadora de Estudos e Projetos (FINEP); Fundação de Amparo à Pesquisa do Estado de Rio de Janeiro (FAPERJ); São Paulo Research Foundation (FAPESP) Grants No. 2019/10151-2, No. 2010/07359-6 and No. 1999/05404-3; Ministério da Ciência, Tecnologia, Inovações e Comunicações (MCTIC); Czech Republic – Grant No. MSMT CR LTT18004, LM2015038, LM2018102, CZ.02.1.01/0.0/0.0/16_013/0001402, CZ.02.1.01/0.0/0.0/18_046/0016010 and CZ.02.1.01/0.0/0.0/17_049/0008422; France – Centre de Calcul IN2P3/CNRS; Centre National de la Recherche Scientifique (CNRS); Conseil Régional Ile-de-France; Département Physique Nucléaire et Corpusculaire (PNC-IN2P3/CNRS); Département Sciences de l'Univers (SDU-INSU/CNRS); Institut Lagrange de Paris (ILP) Grant No. LABEX ANR-10-LABX-63 within the Investissements d'Avenir Programme Grant No. ANR-11-IDEX-0004-02; Germany – Bundesministerium für Bildung und Forschung (BMBF); Deutsche Forschungsgemeinschaft (DFG); Finanzministerium Baden-Württemberg; Helmholtz Alliance for Astroparticle Physics (HAP); Helmholtz-Gemeinschaft Deutscher Forschungszentren (HGF); Ministerium für Kultur und Wissenschaft des Landes Nordrhein-Westfalen; Ministerium für Wissenschaft, Forschung und Kunst des Landes Baden-Württemberg; Italy – Istituto Nazionale di Fisica Nucleare (INFN); Istituto Nazionale di Astrofisica (INAF); Ministero dell'Universitá e della Ricerca (MUR); CETEMPS Center of Excellence; Ministero degli Affari Esteri (MAE), ICSC Centro Nazionale di Ricerca in High Performance Computing, Big Data

and Quantum Computing, funded by European Union NextGenerationEU, reference code CN_00000013; México – Consejo Nacional de Ciencia y Tecnología (CONACYT) No. 167733; Universidad Nacional Autónoma de México (UNAM); PAPIIT DGAPA-UNAM; The Netherlands – Ministry of Education, Culture and Science; Netherlands Organisation for Scientific Research (NWO); Dutch national e-infrastructure with the support of SURF Cooperative; Poland – Ministry of Education and Science, grants No. DIR/WK/2018/11 and 2022/WK/12; National Science Centre, grants No. 2016/22/M/ST9/00198, 2016/23/B/ST9/01635, 2020/39/B/ST9/01398, and 2022/45/B/ST9/02163; Portugal – Portuguese national funds and FEDER funds within Programa Operacional Factores de Competitividade through Fundação para a Ciência e a Tecnologia (COMPETE); Romania – Ministry of Research, Innovation and Digitization, CNCS-UEFISCDI, contract no. 30N/2023 under Romanian National Core Program LAPLAS VII, grant no. PN 23 21 01 02 and project number PN-III-P1-1.1-TE-2021-0924/TE57/2022, within PNCDI III; Slovenia – Slovenian Research Agency, grants P1-0031, P1-0385, I0-0033, N1-0111; Spain – Ministerio de Economía, Industria y Competitividad (FPA2017-85114-P and PID2019-104676GB-C32), Xunta de Galicia (ED431C 2017/07), Junta de Andalucía (SOMM17/6104/UGR, P18-FR-4314) Feder Funds, RENATA Red Nacional Temática de Astropartículas (FPA2015-68783-REDT) and María de Maeztu Unit of Excellence (MDM-2016-0692); USA – Department of Energy, Contracts No. DE-AC02-07CH11359, No. DE-FR02-04ER41300, No. DE-FG02-99ER41107 and No. DE-SC0011689; National Science Foundation, Grant No. 0450696; The Grainger Foundation; Marie Curie-IRSES/EPLANET; European Particle Physics Latin American Network; and UNESCO.